IJSES
International Journal of Scientific Engineering and Science
Volume 9, Issue 3, pp. 20-36, 2025.
ISSN (Online): 2456-7361

Maximum Power Point Tracking Based on Modified Firefly Algorithm for PV System under Partial Shading Conditions

Mana Abusaq[1*], Mohamed A. Zohdy[2]
[1,2]Department of Electrical and Computer Engineering, Oakland University, Rochester, MI 48309, USA
*Corresponding author: abusaq@oakland.edu

Abstract— *Photovoltaic (PV) systems subjected to partial shading condition (PSC) can extremely decrease their output power. Therefore, it is essential to establish a robust mechanism capable of continuously monitoring and accurately tracking the maximum power output, even under dynamic and fluctuating conditions. There are various maximum power point tracking (MPPT) control algorithms designed to counteract the shading effects. The aim of this paper is to study the performance of the MFA for photovoltaic MPPT under PSCs. To validate the study, comparative analysis of four algorithms namely, P&O, PSO, FA, and MFA is conducted, and results demonstrate the superiority of the MFA algorithm over the other algorithms. Additionally, the effect of the load resistance on the performance of the above mentioned MPPT algorisms has been carried out. A comprehensive performance evaluation of the aforementioned algorithms was performed in MATLAB/Simulink software tool. Three patterns of PSC have been considered during the study namely: middle peak, left peak, and right peak. In each of those scenarios, the performance of each algorithm has been evaluated, and comparison was conducted among those methods. The results show that MFA is the most efficient and adaptive algorithm for optimizing power extraction in PV systems under varying shading and load conditions*.

Keywords— *Maximum power point tracking, PV system, Partial shading conditions, Modified firefly algorithm.*

I. INTRODUCTION

Currently, electrical energy has become an essential component worldwide to provide better living standards. It plays a crucial role in supporting all other vital facets of civilization. Conventional energy sources such as oil and coal leads to increased cost of fossil fuels, environmental factors, and their effects on human health. Researchers find better alternatives to reduce the consumption amount of fossil fuels. There are various alternatives for generating pollution-free electricity by means of sustainable energy sources. Sustainable energy sources denote naturally occurring types such as wind, biomass, solar, fuel cells, and water, acknowledged for being clean and limitless. Among the various sustainable energy sources, solar energy is mainly used for generating electrical power due to its lower maintenance and minimal operational expenses. The advancement of solar energy collection has recently garnered increased focus and is primarily employed for both stand-alone and grid-connected systems [1], [2].

When sun irradiance and ambient temperature fluctuate, photovoltaic (PV) systems' output power changes nonlinearly. Traditional approaches for maximum power point tracking (MPPT) include fractional open circuit voltage (FOCV), fractional short circuit current (FSCC), incremental conductance (INC), and perturb and observe (P&O). However, when a photovoltaic system is in partial shading condition (PSC), the most shaded cell may limit the current of a string of cells connected in series. This can result in the hot-spot problem, which happens when the most shaded cell becomes reverse-biased by the other cells, potentially causing destructive heating. In order to address the hot-spot problem, bypass diodes are usually connected in parallel to the cell cluster. This, however, results in numerous local maximum power points (LMPPs) in the power-voltage (P-V) curve and multiple-step patterns in the string's current-voltage (I-V) curve due to the additional bypass diodes. Because of this, traditional MPPT algorithms may often be unable to determine the global maximum power point (GMPP) among the many LMPPs, which would prevent the PV system from operating at its full potential [3].

Thus, choosing a proper control method is necessary to achieve the GMPP. Fuzzy logic, neural networks (NNs), normal harmonic search (NHS), and Cauchy and Gaussian sine cosine optimization (CGSCO) are examples of soft computing-based methods that have been effectively applied to find the best operating points for PV systems under PSCs. Furthermore, a number of nature-inspired algorithms have also been shown to perform well for MPPT applications under PSCs, including the firefly algorithm (FA), genetic algorithm (GA), differential evolution (DE), grey wolf optimization (GWO), intelligent monkey king evolution algorithm (IMKE), and particle swarm optimization (PSO) [4]. In addition, hybrid nature-inspired algorithms, such as the hybrid GA & FA, GWO with P&O, hybrid Jaya & DE (JayaDE), and whale optimization with DE (WODE), could offer better responses with higher tracking accuracy than their individual antecedents. As Compared to the conventional methods utilized in PSCs, the above mentioned Meta-heuristic algorithms methods have multiple advantages like auto identification of the shadow patterns, search for the GMPP, and having a simple structure [5], [6]. To track the MPP, few articles have recently used enhanced techniques such modified perturbation and observation. They can monitor the worldwide MPP. These approaches differ in terms of precision, speed, and intricacy. These methods are slow even though they can follow the MPP well [7].

The dividing rectangles algorithm was employed by the authors in [8] for the MPPT under PSC. The PV module's P-V characteristic curve fully matches the Lipschitz function using

International Journal of Scientific Engineering and Science
Volume 9, Issue 3, pp. 20-36, 2025. ISSN (Online): 2456-7361

this method. This approach can therefore be used to determine the highest value. An adaptive Neuro-fuzzy inference system-based MPP tracker for PV modules is proposed in [9]. The tracking MPP is unable to track the global MPP in PSC when it is in uniform irradiance circumstances. An adaptive neuro-fuzzy inference system was proposed in [10]as an MPPT for PV systems. The incremental conductance method based on the uniform irradiance approach was utilized to train ANFIS. In [11], the MPPT application was done using a hybrid approach. The first stage uses the ACO algorithm to get close to the MPP, and the P&O approach is then used to follow the MPP.

The author of [12] employed the ABC algorithm for MPPT. To match the PV system and the output load, a boost converter was used. The suggested method's speed was shown to be higher when compared to the improved P&O and PSO approaches. In order to enhance its exploration capabilities, the DE algorithm was combined with the PSO algorithm [13]. In the known combined PSO-DE method, the PSO algorithm is in charge of half of the iterations, while the DE algorithm is in charge of the other half. In other words, the DE algorithm takes over for the subsequent iteration once the PSO runs for the first one. This keeps happening until the termination condition is met. In terms of efficiency, tracking speed, simplicity, and oscillations around the MPP, the hybrid PSO-DE approach outperforms incremental conductance, fuzzy logic controller, and PSO techniques, as demonstrated by the simulation data presented in the research.

In this paper, the performance evaluation and comparison of MPPT algorithms, including P&O, PSO, FA, and the Modified Firefly Algorithm (MFA), for a PV system operating under various partial shading conditions has been conducted. The aim of this paper is to study the performance of the MFA for photovoltaic MPPT under PSCs. Additionally, we examined the impact of load resistance on the performance of the metaheuristic algorithms used in this study. To validate the study, we have conducted those comparisons which show the superiority of our MFA over the other algorithms. The comparative analysis has been carried out using MATLAB/Simulink software.

II. Characteristic of Solar Cells

A cell may alter the short circuit current from mill amperes to several amps, and the voltages it produces are around half of the nominal light intensity. The nominal generation capacity of the cell can be ascertained by multiplying the open circuit voltage by the short circuit current, which yields the maximum generation capacity of the cell. Typically, a cell's power output ranges from a few mill watts to several watts [14].

$$I = I_{pv} - I_0[exp(\frac{V - R_s I}{V_t a}) - 1] - \frac{V + R_s I}{R_{sh}} \quad (1)$$

Where I_{PV} is the produced current of photovoltaic and I_0 is the reverse saturation current. ($V_t = N_s KT/q$) is thermal voltage of the photovoltaic array where they are connected in series with N_s cells, q is the electron charge (q = 1.6e^{-19}c) and T is cell's temperature in Kelvin. K is Boltzmann factor (K=1.3805e^{-23}j/k) and "a" is diode's ideal constant. The equivalent circuit of the solar PV module is depicted in the Fig.1.

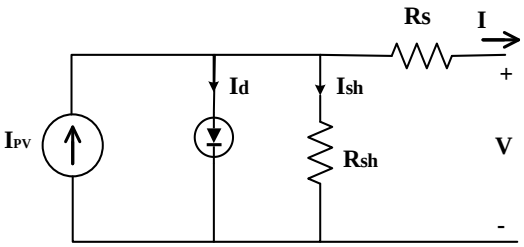

Fig. 1. Equivalent electrical model of solar PV module.

III. Characteristics of Pv Module Under PSC

Solar photovoltaic system is one of the most promising power systems based on renewable energy sources, with several advantages compared to others. However, solar PV systems have a challenge of low conversion efficiency because most of the irradiances of the sun, which are channeled to the PV panels, are not fully utilized for power consumption. A more complex challenge arises in the system when certain PV panels are partially obstructed from receiving full solar irradiance, a phenomenon known as Partial Shading Conditions (PSCs) in solar PV systems. This shading effect results in the formation of multiple LMPPs in the P-V characteristics. The presence of multiple peaks, especially in arrays with extended series connections, significantly increases the complexity of the P-V curve, making it more difficult to accurately track the true GMPP [15], [16]. The power produced by PV modules may be greatly reduced under such circumstances since traditional MPPT conditions and methods may fail to distinguish between LMPPs and GMPPs with ease and may become locked at a local peak. Additionally, the radiation intensity is likely to fluctuate quickly, which could result in variations in the GMPP's location and curve pattern. Consequently, in order to obtain the system's maximum power output, the authorized MPPT algorithm must be able to swiftly and accurately detect GMPP among the LMPPs under PSCs [17].

The photovoltaic system's P-V and P-I curves for both variable and uniform irradiances are displayed in Fig. 2.

Irradiation Patterns:

This work examines three different irradiation scenarios pertaining to partial shading: middle peak, left peak, and right peak. The following consecutive figures show the three scenarios.

- *Middle Peak*

In this case, the irradiance levels provided to the three PV panels are 1000 W/m², 700 W/m², and 300 W/m² for PV-1, PV-2, and PV-3, respectively. There are three distinct peaks located at three different point of operation.

International Journal of Scientific Engineering and Science
Volume 9, Issue 3, pp. 20-36, 2025. ISSN (Online): 2456-7361

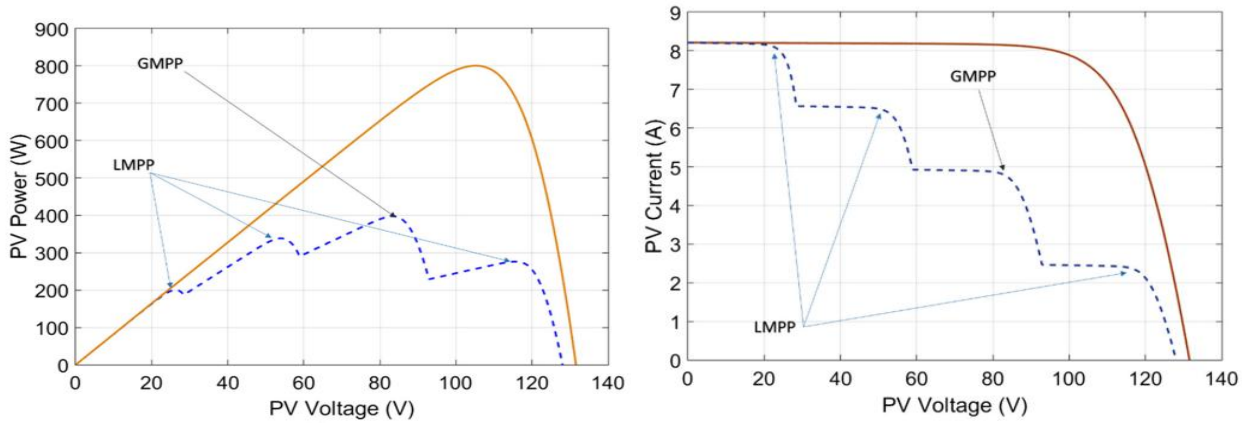

(a) (b)

Fig. 2. (a) P–V curve, (b) I-V curve under PSC and uniform irradiance [18].

The GMPP of the three occurs in the middle peak as shown in Fig. 3.

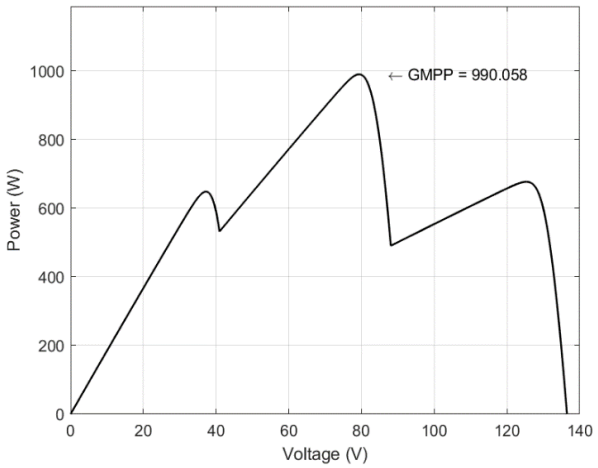

Fig. 3. Middle peak irradiation pattern.

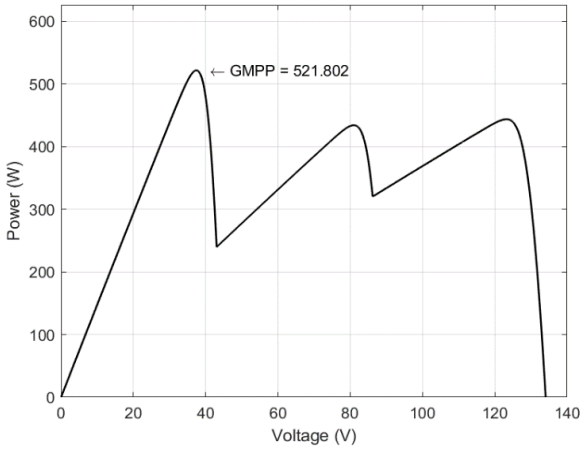

Fig. 4. Left peak irradiation pattern.

- *Left peak*

The left peak occurs when the irradiance levels at PV-1, PV-2, and PV-3 are 800 W/m², 300 W/m², and 200 W/m², respectively. Such a condition causes three peaks similar to the previous case but the global maximum power point occurs at the left-most of those three points. For the specific values of solar irradiation used in this simulation the maximum power that can be generated is around 521.802 W, as depicted in Fig. 4.

- *Right peak*

For the third case in which the GMPP is located on the right, the following solar irradiation values were used, 500 W/m^2 for PV-1,700 W/m^2 for PV-2 and 900 W/m^2 for PV-3. Fig. 5 shows the panel power versus voltage curve where the GMPP is indeed located to the right side. In this case the reached GMPP is approximately 1101.58 W.

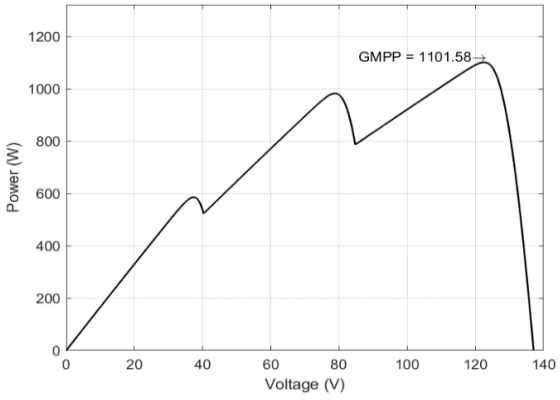

Fig. 5. Right peak irradiation pattern.

IV. Perturbation And Observation Algorithm

The most common MPPT algorithm is P&O, mainly due to its acceptable performance and low complexity [19]. It achieves MPP tracking by introducing perturbations to a single variable, usually the voltage. Based on the criteria for tracking, a perturbation is applied to the operating voltage of a PV system by changing the duty cycle. This causes the generated power of a PV system to be increased, it means that the operating point moves toward the MPP. Consequently, the productive perturbation is formed in the same direction. This procedure will continue until the MPP is reached. However, if the attained PV system is reduced, it means that it is moving away from the

International Journal of Scientific Engineering and Science
Volume 9, Issue 3, pp. 20-36, 2025. ISSN (Online): 2456-7361

MPP and as a result, direction of the produced perturbation must be reversed [20], [21].

Even though this method is pretty straightforward, its efficiency highly depends on the convergence speed. The difficulty of P&O method is because of its high fluctuation around the MPP due to inability in precise tracking of the MPP. Hence, the output always experiences fluctuations and this leads to the loss of energy [22]. Performance of the P&O method degrades with the changes in environmental conditions, i.e., during cloudy days, and the reason behind it is that this method faces challenges in accurately tracking the GMPP under PSC [23], [24].

V. Particle Swarm Optimization (PSO) Algorithm

PSO is a population-based evolutionary search algorithm. This method maintains a swarm of particles and each particle represents a potential solution in the swarm [14], [25]. PSO identifies the optimal parameters that either maximize or minimize the objective function within a defined search space. Each particle within the swarm maintains a current position, velocity, and a personal best position within the search space. The personal best position, *pbesti,* represents the location where a particle has achieved the highest value based on the objective function *F*, particularly in a maximization scenario. Additionally, the position corresponding to the highest value among all personal bests is termed the global best position, denoted as *gbesti* [26].

Upon identifying optimal solutions, the particles adjust their accelerations and positions based on the predefined equations.

$$V_i^{k+1} = WV_i^k + C_1 rand_1^k\left(pbest_i^k - X_i^k\right) + C_2 rand_2^k\left(gbest_i^k - X_i^k\right) \quad (2)$$

$$X_i^{k+1} = X_i^k + V_i^{k+1} \quad (3)$$

where V_i^k denotes acceleration of the particle *i* after *k* times of iterations, *W* is the weight, C_1 and C_2 are the acceleration constants for moving toward each individual or global best experiences, respectively, and $rand_1$ and $rand_2$ are random numbers between 0 and 1.

VI. Firefly Algorithm (FA)

FA is metaheuristic optimization algorithm inspired by the social behavior of fireflies developed by Yang in 2008 [6]. It is intelligence-based algorithm inspired by the flashing fireflies to attract mating partners and potential prey that is common in the summer sky of tropical temperate zones. The basic idea of formulation of the algorithm is the attractiveness of fireflies that the less bright one will be attracted to the brighter one [17].

The firefly algorithm has three main assumptions which are derived from firefly features:

1) Fireflies are not gender-specific, meaning they are naturally attracted to individuals with higher brightness regardless of gender. They move toward the brighter fireflies based on their perceived intensity.
2) The attractiveness of a firefly is directly proportional to its brightness, which decreases as the distance between fireflies increases. If no firefly appears brighter or more attractive, movement occurs randomly within the search space.
3) The brightness or attractiveness of each firefly is determined by the value of the objective function, which influences its movement and guides the search process toward optimal solutions.

Based on the three rules mentioned above, the execution process of the firefly algorithm for MPPT in a PV system is shown in Fig 6:

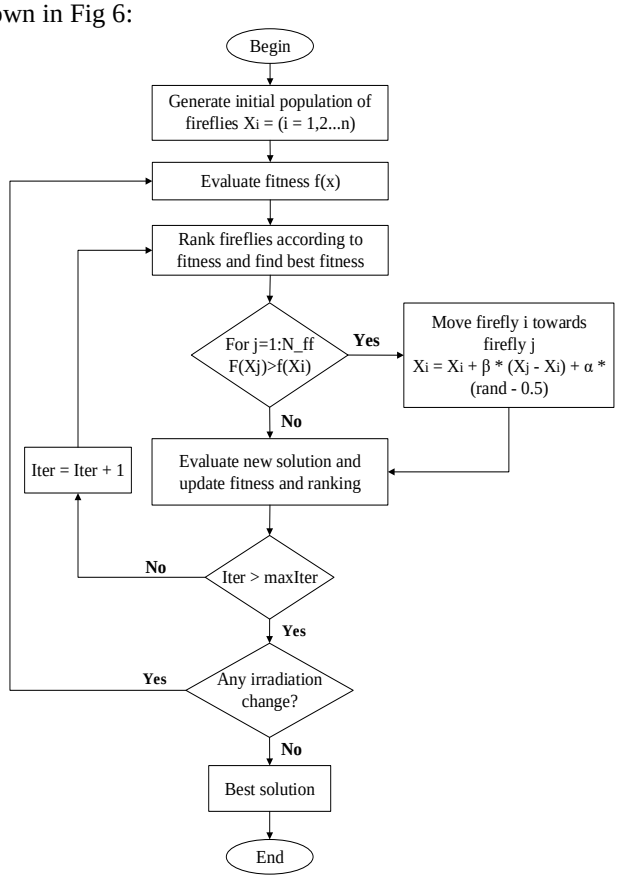

Fig. 6. Flowchart for the FA.

Since the attraction of a firefly is directly proportional to the light intensity seen by the nearby firefly, the parameter β as the attractiveness can be defined as follows:

$$\beta = \beta_0 e^{-\gamma r^2} \quad (4)$$

Where β_0 is attractiveness at $r = 0$. The distance between fireflies *i* and *j* located at X_i and X_j coordinates is calculated as:

$$r_{ij} = \left\|X_i - X_j\right\| = \sqrt{\sum_{K=1}^{d}\left(X_{i,k} - X_{j,k}\right)^2} \quad (5)$$

Where $X_{i,k}$ is kth component of X_i related to firefly *i*. The movement of firefly *i* towards a more attractive firefly *j* is defined as below:

$$X_i^{t+1} = X_i^t + \beta_0 e^{-\gamma r^2}\left(X_j - X_i\right) + \alpha\varepsilon_i \quad (6)$$

Where the second expression corresponds to the attraction, while the third term, $\alpha\varepsilon_i$, represents the randomizer parameter, α is the coefficient of randomizer parameter, and ε_i is a random vector comprising of numbers obtained from a Gaussian or uniform distribution.

International Journal of Scientific Engineering and Science
Volume 9, Issue 3, pp. 20-36, 2025. ISSN (Online): 2456-7361

VII. Modified Firefly Agorithm (MFA)

One of the primary limitations of FA is that its coefficients remain fixed throughout the iterations, preventing them from adapting dynamically over time. This rigidity limits the algorithm's ability to optimize effectively in changing conditions. Additionally, FA does not retain historical data, which could be valuable for guiding future iterations. These constraints necessitate the development of an improved version, known as MFA.

MFA is designed to address these limitations by enhancing both exploitation and exploration within the search space. Unlike the original FA, where key parameters such as randomization and attractiveness remain static, MFA dynamically adjusts these values during optimization. This modification allows for improved local exploration, ensuring more effective searches near local optima while maintaining the ability to progress toward the global optimum. By refining the search process, MFA reduces unnecessary randomness and stagnation, leading to a more structured and efficient convergence.

Another significant advantage of MFA is its ability to accelerate the movement toward the optimal solution. By expanding the movement range of fireflies in a more controlled manner, the algorithm enhances its capacity to navigate complex optimization landscapes. The mathematical formulation used to refine firefly movement is expressed as [27]:

$$X_{i+1} = \beta(t) X_i + X_j (1 - \beta(t)) + \alpha(t) \varepsilon_i \quad (7)$$

Where ε_i represents the random number, $\beta(t)$ represents attractiveness coefficient, the time t, and the $\alpha(t)$ denotes randomness coefficient at time (t).

The parameters in conventional FA may result in varying performances when solving optimization problems. Manually tuning the parameters of FA for different optimization problems with varying characteristics is a challenging task. To overcome this limitation and prevent premature convergence, MFA introduces an adaptive strategy for parameter selection. This approach is crucial in dynamically adjusting the randomization coefficient to maintain a balance between exploration and exploitation throughout the optimization process. The adaptive randomness coefficient α is formulated as [27]:

$$\alpha(Itr_i) = exp\left(1 - \left(\frac{Itr_{max}}{Itr_{max} - Itr_i}\right)^c\right) \quad (8)$$

where c represents an integer value that determines the rate at which randomness decays over iterations. Itr_{max} denotes the maximum number of iterations allowed in the optimization process, while Itr_i corresponds to the current iteration number

Furthermore, the parameter γ is essential in regulating convergence speed and attractiveness, influencing the balance between exploration and exploitation in the optimization process, as given in [27]:

$$\gamma(Itr_i) = 1 - exp\left(1 - \left(\frac{Itr_{max}}{Itr_{max} - Itr_i}\right)^c\right) \quad (9)$$

The proposed modified firefly algorithm avoids being trapped in local extrema while accelerating convergence, ensuring a balanced search between local and global optima.

To further enhance search capabilities, a heterogeneous updating rule based on Gray Relational Analysis (GRA) is applied, which is effective for handling incomplete information in finite sequences. In the search process, two updating equations are randomly selected and implemented, as presented in (10) [27]:

$$X_{i+1} = \begin{cases} \beta(t) Xi + Xj(1 - \beta(t)) + \alpha(t) \varepsilon i & rand > 0.5 \\ \frac{NG - i}{NG}(1 - \delta) X_i + \delta X_{best} & ELSEWHERE \end{cases} \quad (10)$$

Where δ represents the gray coefficient and NG is the number of generations.

VIII. Application of MFA to MPPT

The use of MFA in tracking the MPP under PSC is described in this section. The execution process and the block diagram of the MPPT scheme based on the MFA approach in a PV system are displayed in Fig. 7 and Fig. 8 respectively. Three photovoltaic modules are connected in series in the planned system. Additionally, the load and the PV system are interfaced via a DC-DC boost converter.

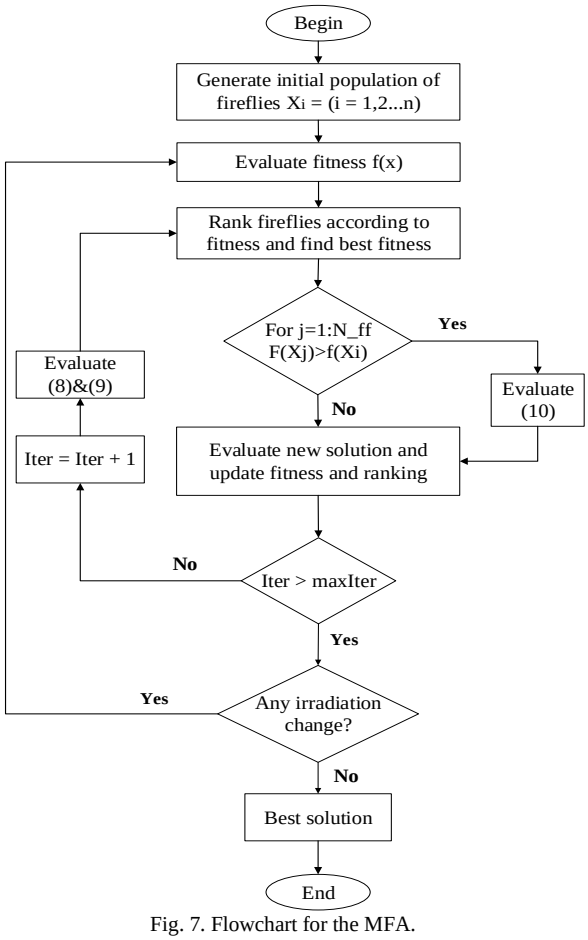

Fig. 7. Flowchart for the MFA.

International Journal of Scientific Engineering and Science
Volume 9, Issue 3, pp. 20-36, 2025. ISSN (Online): 2456-7361

The steps of the MFA algorithm toward MPPT are described as follows:

Step 1: Initialize Parameters:

Define the key MFA constants, including β_0 (attraction factor), δ (mutation factor), c (adaptation control), γ (light absorption factor), maximum iterations, and firefly population size (N_ff). Firefly positions represent duty cycle values and their brightness corresponds to power output.

Step 2: Initialize Firefly Positions:

Fireflies are randomly placed within the duty cycle (d_{min}= 0.1 to d_{max}= 0.9). Each firefly's intensity (power) is initialized, along with a randomly assigned best firefly position.

Step 3: Evaluate Firefly Brightness:

Each firefly's duty cycle is applied to the system, and the corresponding power output is measured. The brightness (fitness) of each firefly is determined by its power output. The iteration counter is incremented.

Step 4: Update Firefly Positions:

Fireflies update their positions based on (10), Moving towards the brightest firefly. The parameters α and γ are also updated using (8) and (9) to improve convergence.

Step 5: Rank Fireflies and Identify Best Solution:

Fireflies are ranked based on their brightness. The firefly with the highest intensity is set as the new best firefly (X_{best}), and its duty cycle is stored as the optimal candidate.

Step 6: Check Stopping Condition:

If the iteration count reaches the predefined limit ($Itr > Itr_{max}$), the process stops, and the current best duty cycle is recorded as the final solution. If not, the algorithm continues.

Step 7: Update Adaptive Parameters:

If the stopping conditions is not met, α and γ are updated dynamically using (8) and (9) to refine firefly movement and improve optimization.

Step 8: Check for Irradiance Change:

Before the next iteration, the algorithm checks if the irradiance level has changed. If a change is detected, fireflies are reinitialized, and the process returns to *step 2*. If no change occurs, the algorithm returns to *step 3*.

Step 9: Repeat until Convergence:

The process returns to *step 3* and continues iterating until the stopping conditions is met.

Step 10: Store the Optimal MPP:

Once the stopping condition is satisfied, the optimal duty cycle and corresponding maximum power output are stored. The process then terminates.

The simulation and model components along with their parameter values used in this work are listed in TABLE I.

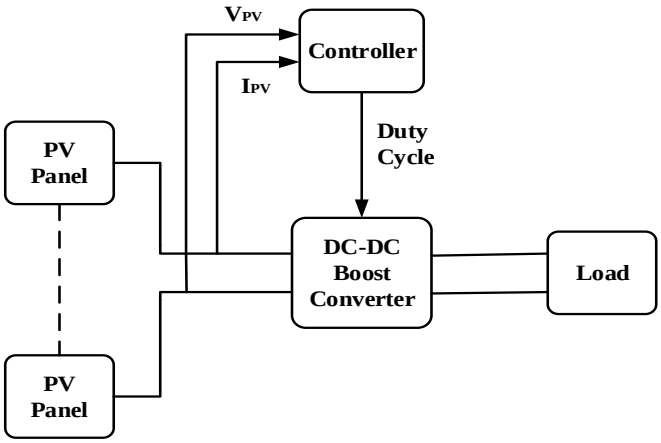

Fig. 8. The tracking scheme based on PSO, FA, and MFA methods.

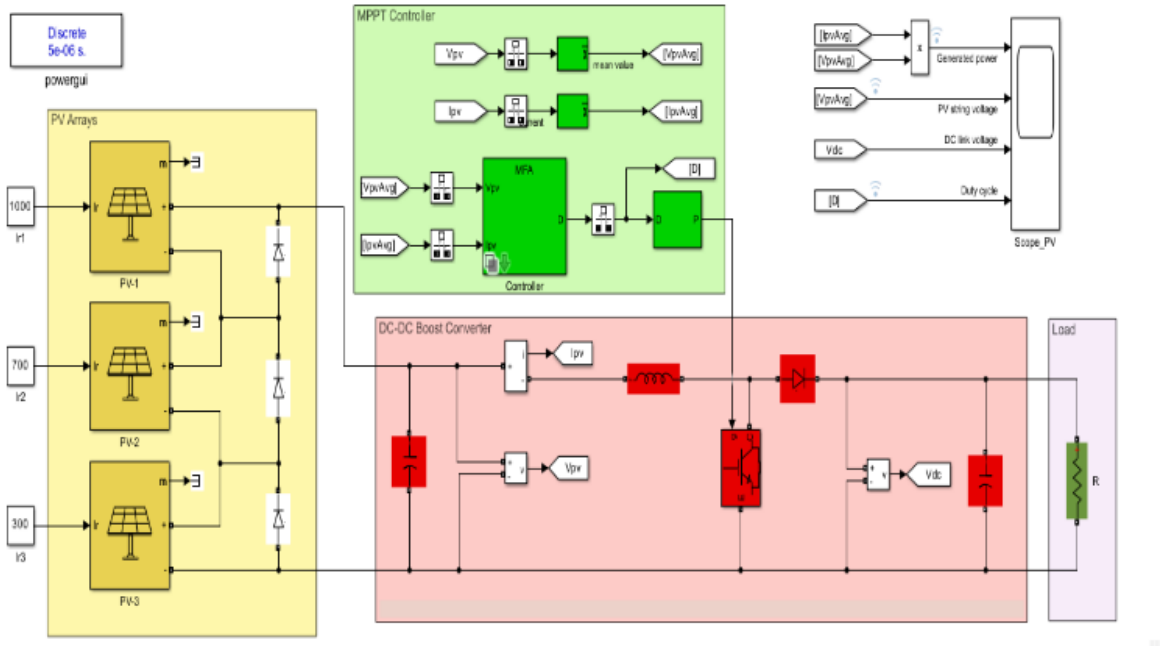

Fig. 9. MATLAB/Simulink simulation of the P&O, PSO, FA, and MFA based MPPT system.

International Journal of Scientific Engineering and Science
Volume 9, Issue 3, pp. 20-36, 2025. ISSN (Online): 2456-7361

TABLE I. System model and controller parameters.

System	Parameter	Description	Value
PV module	N_{cell}	Cells per module	132
	V_{oc} (V)	Open circuit voltage	45.7
	I_{sc} (A)	Short circuit current	18.53
	P_{max} (W)	Maximum power	660.366
	V_{mp} (V)	Voltage at MPP	37.8
	I_{mp} (A)	Current at MPP	17.47
P&O	d_{max}	Maximum duty ratio	0.9
	d_{min}	Minimum duty ratio	0.1
	ΔD	Change in duty	$5*10^{-7}$
PSO	ω	inertia	0.1
	$C1$	Self-adjustment weight	2
	$C2$	Social-adjustment weight	0.4
	Np	Number of particles	5
	lb	Lower bound	0.1
	ub	Upper bound	0.9
	$Iter_{max}$	Maximum number of iterations	20
FA	α	Coefficient of randomizer	0.9
	β_0	Attractiveness coefficient	1.9
	γ	Light absorption coefficient	1.9
	N_ff	Number of fireflies	100
	lb	Lower bound	0.1
	ub	Upper bound	0.9
	$Iter_{max}$	Maximum number of iterations	20
MFA	α	Coefficient of randomizer	0.9
	β_0	Attractiveness coefficient	1.9
	γ	Light absorption coefficient	1.9
	C	Speed of decaying of the randomness	1.0
	δ	Gray coefficient	0.8
	N_ff	Number of fireflies	100
	lb	Lower bound	0.1
	ub	Upper bound	0.9
	$Iter_{max}$	Maximum number of iterations	20
Boost Converter	$L(mH)$	Inductance	0.9
	C_{in} (μF)	Input capacitance	1.9
	C_{out} (μF)	Output capacitance	1.9
Simulation	Ts (μs)	Sampling time	1.0
	fs (kHz)	Switching frequency	0.8

IX. Simulation Results

The simulation model used to study the performances of the algorithms is setup as shown in Fig. 9. It consists of three solar PV panels connected in series each with its own solar irradiance input to simulate partial shading, a boost DC-DC converter, a resistive load and an MPPT controller with options of P&O, PSO, FA and MFA algorithms that output duty ratio to a PWM generator which controls the boost converter IGBT.

- *Middle Peak*

In the middle peak condition discussed earlier (i.e. PV-1 at 1000W/m^2, PV-2 at 700W/m^2, and PV-3 at 300W/m^2), four of the MPPT algorithms were tested for a load resistance of 20Ω

Fig. 10 shows such a simulation in which the three PVs were under middle peak condition and the MPPT controller is P&O. In Fig.10 (a), it is observed that the P&O algorithm reaches the maximum power at 939.73W and remains stable for the rest of the simulation.

The performance of the PSO algorithm with regard to tracking maximum power is depicted in Fig. 11. Fig. 11 (b) shows that the algorithm searches for the duty ratio corresponding to maximum power for the first 2 seconds, 20 iterations, and settles on around d = 0.31 giving about 940.29W of output power.

In Fig.12, the power output of the PVs and the duty ratio for FA are shown. The power generated in this case is 829.89W and the duty ratio is around 0.45. It is clear that the algorithm is not efficiently tracking the GMPP.

The power output of the PVs and the duty ratio for the MFA are depicted in Fig.13. After the maximum number of iterations are reached, the duty ratio settles around d = 0.38 and the power output is about 940.29W which is the same as the PSO controlled system.

The power outputs of the PVs under the middle-peak shading pattern, controlled by the four algorithms, are plotted together for comparison in Fig.14. It is observed that both the PSO and MFA algorithms show better MPP tracking capability than the other two algorithms (P&O and FA). In terms of convergence speed the MFA seems to reach the peak power value faster than the PSO algorithm. In this case the P&O algorithm resulted in better MPP tracking performance than the FA algorithm. All of the heuristic algorithms, PSO, FA, and MFA, were designed to have maximum number of iterations of 20. Since those algorithms update every 0.1 seconds, all of them stop searching for better solutions when the simulation time reaches 2 seconds.

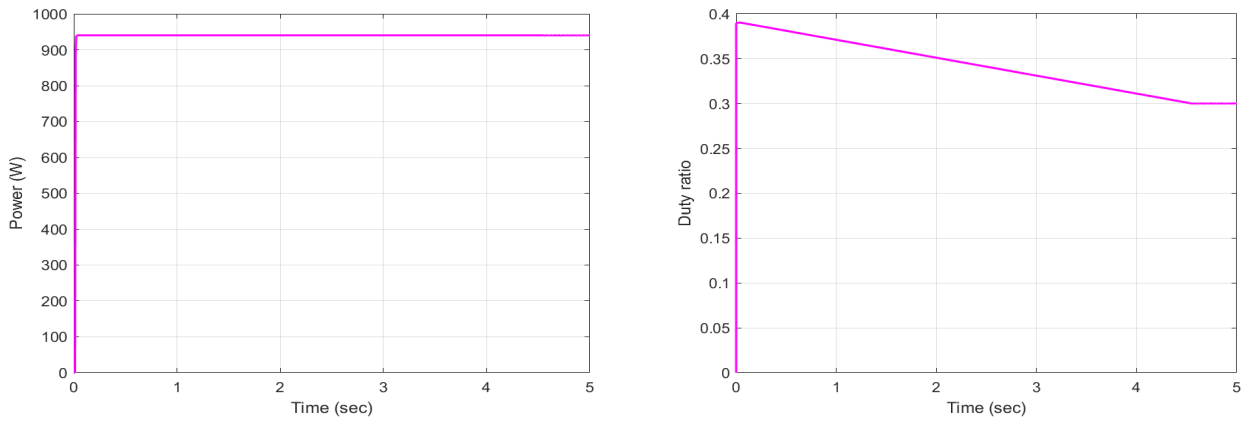

(a) PV power output (b) PWM duty ratio

Fig. 10. Middle-peak P&O performance.

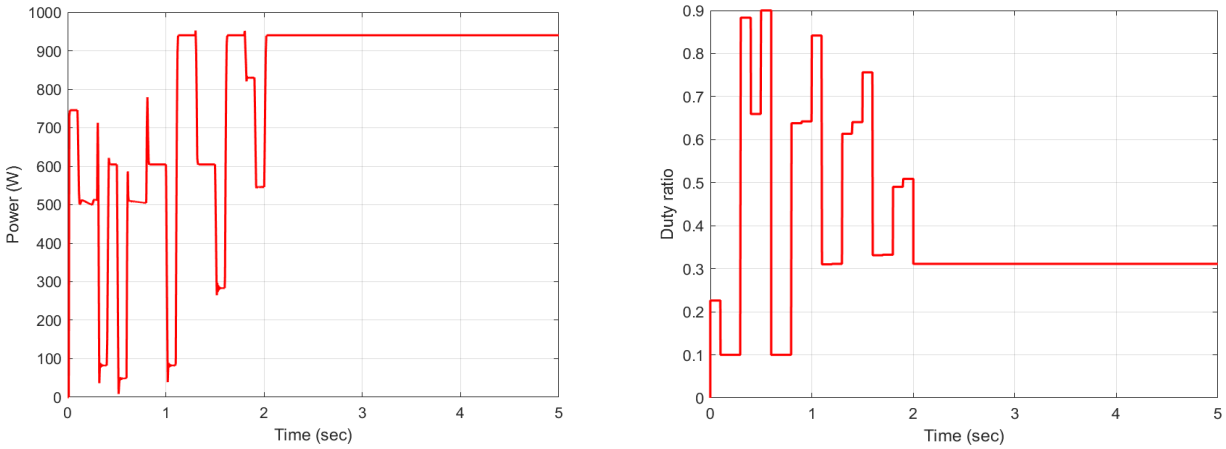

(a) PV power output (b) PWM duty ratio

Fig. 11. Middle-peak PSO performance.

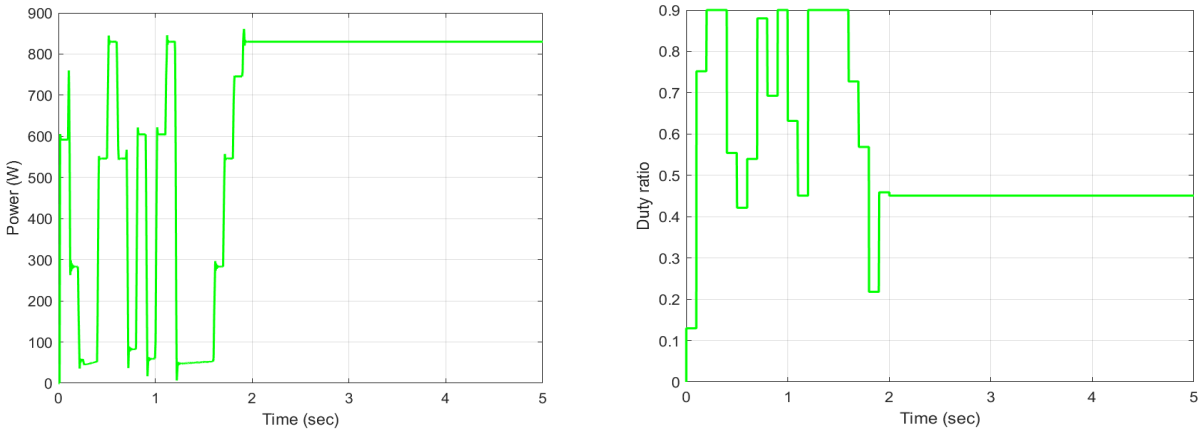

(a) PV power output (b) PWM duty ratio

Fig. 12. Middle-peak FA performance.

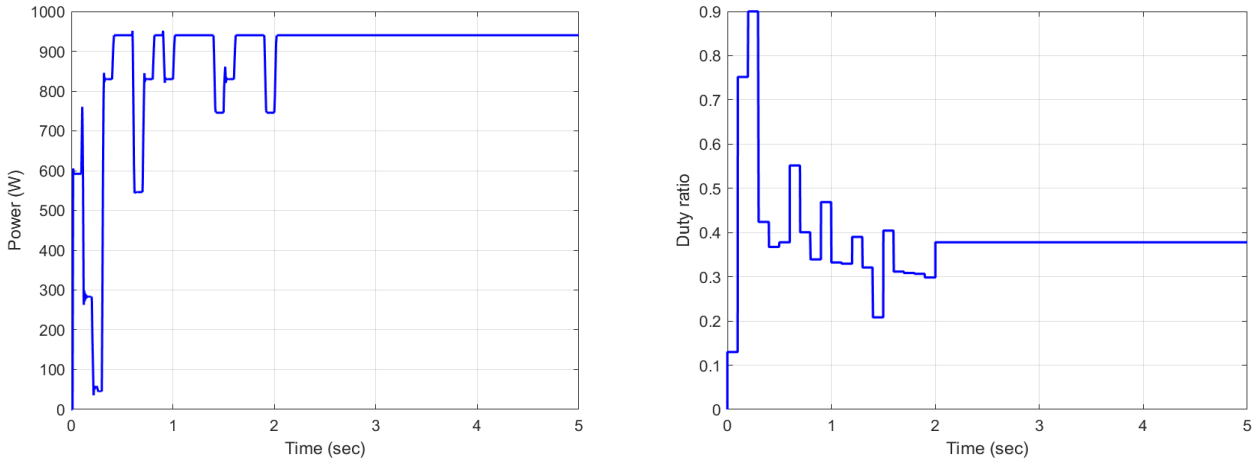

(a) PV power output (b) PWM duty ratio

Fig. 13. Middle-peak MFA performance.

International Journal of Scientific Engineering and Science
Volume 9, Issue 3, pp. 20-36, 2025. ISSN (Online): 2456-7361

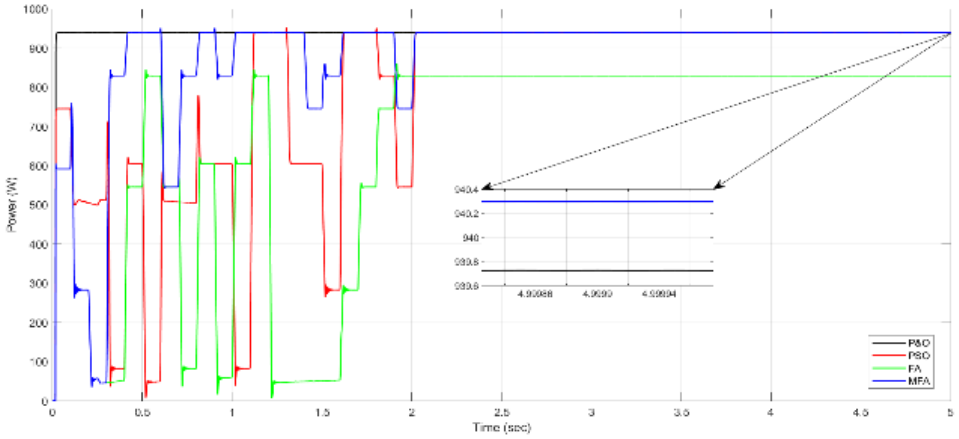

Fig. 14. Comparison of algorithms for middle peak.

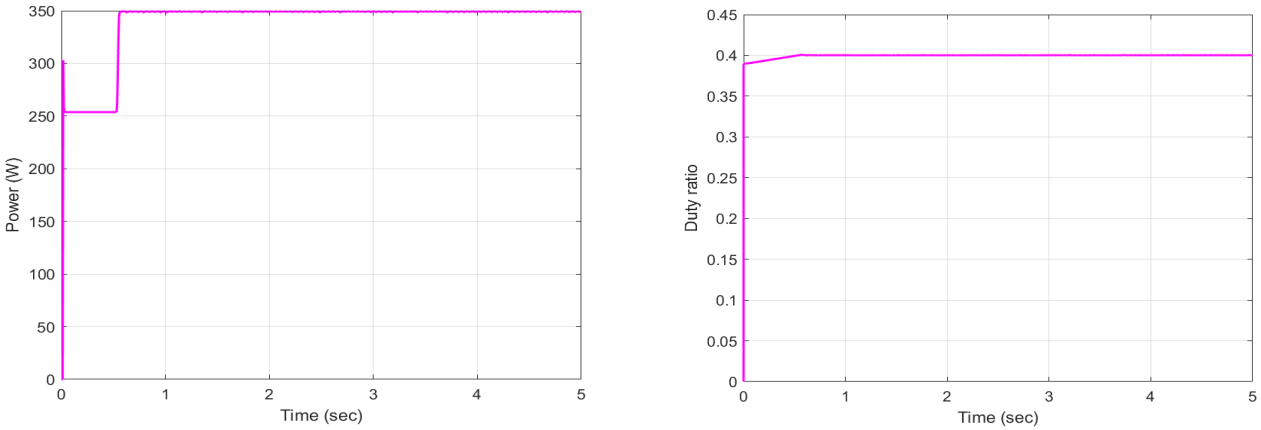

(a) PV power output (b) PWM duty ratio

Fig. 15. Left-peak P&O performance.

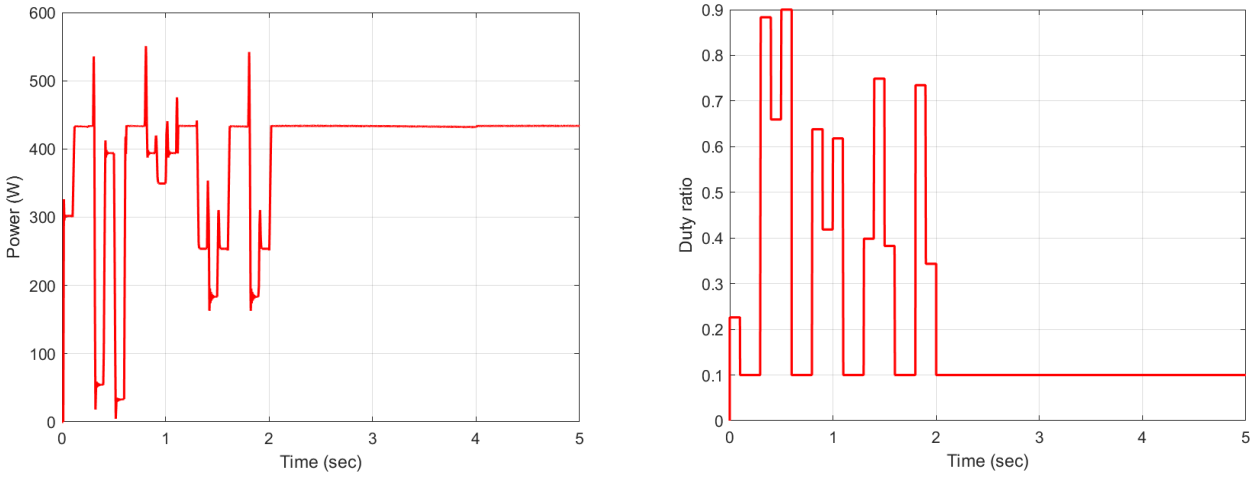

(a) PV power output (b) PWM duty ratio

Fig. 16. Left-peak PSO performance.

- *Left Peak*

Is this case, the left peak in the GMPP is located at the left-most peak point of the three peaks. Similar to the previous cases in the middle peak, the three PVs were exposed to different levels of solar irradiation representing partial shading by setting the irradiance level of PV-1 at 800W/m^2, PV-2 at 300W/m^2, and PV-3 at 200W/m^2. By running the simulation for the four MPPT algorithms the results depicted in the figure were obtained.

Fig. 15 shows such a simulation in which the three PVs were under left peak condition and the MPPT controller is P&O. In

Volume 9, Issue 3, pp. 20-36, 2025. ISSN (Online): 2456-7361

Fig 15 (a), it is observed that the P&O algorithm reaches the maximum power of 348.67W approximately 0.5 seconds and stays there for the rest of the simulation.

The performance of the PSO algorithm in tracking maximum power is illustrated in Fig. 16. The algorithm initially searches for the optimal duty ratio corresponding to the maximum power output during the first 2 seconds, completing 20 iterations. It then stabilizes at a duty ratio of approximately $d = 0.1$, yielding an output power of 433.78W.

Fig. 17 presents the performance of the PVs for the FA algorithm. In this case, the generated power reaches 487.53W, with the duty ratio stabilizing around $d = 0.54$.

Fig. 18 illustrates the power output and the duty ratio of the PVs when applying the MFA controller. The observed performance is closely similar to that in FA. The generated power reaches 487.53W, while the duty ratio stabilizes around $d = 0.54$.

The comparison of the four algorithms for the left peak shading pattern is plotted here in Fig. 19, and it can be concluded that the FA and MFA algorithms deliver better MPP tracking performance than the other two algorithms. The other main point is that the MFA reaches the optimal duty cycle faster than the other algorithms.

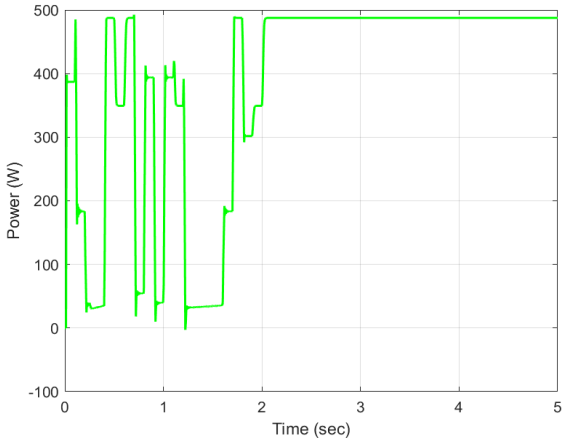

(a) PV power output

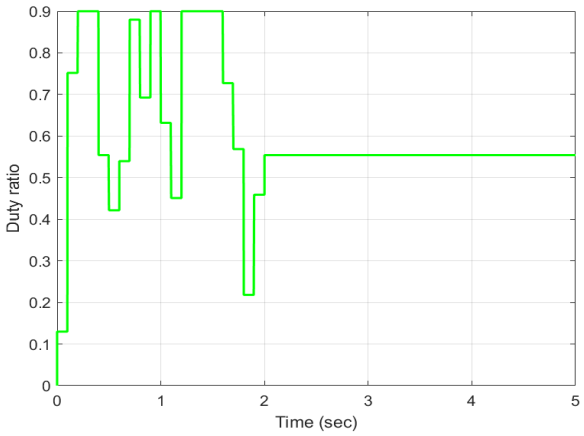

(b) PWM duty ratio

Fig. 17. Left-peak FA performance.

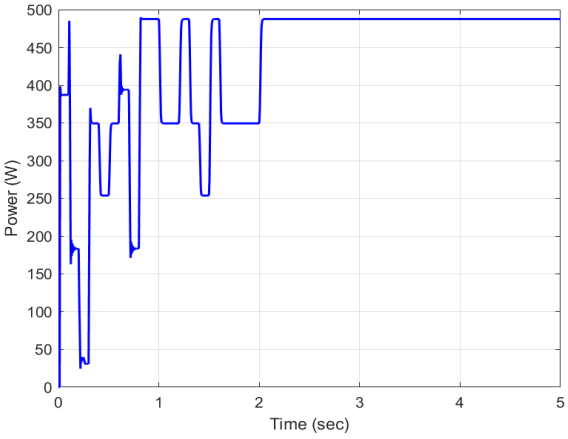

(a) PV power output

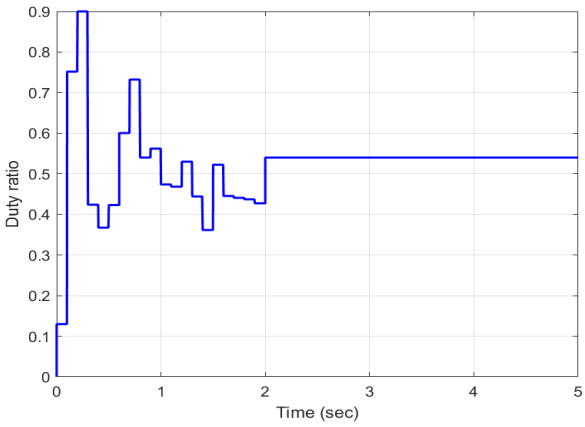

(b) PWM duty ratio

Fig. 18. Left-peak MFA performance.

- *Right Peak*

In this condition, simulation results of the four algorithms when subjected to the right peak condition are presented. Fig. 20 shows the simulation result of P&O algorithm in which the three PVs were under right peak condition. It is observed that the P&O algorithm reaches the maximum power of 931.45W and retains this value for the rest of the simulation.

Fig. 21 illustrates the performance of the PSO algorithm in tracking the maximum power point. The algorithm initially searches for the optimal duty ratio corresponding to maximum power over the first 2 seconds, completing 20 iterations. Eventually, it converges to a duty ratio of approximately $d = 0.1$, achieving an output power of 1.051KW

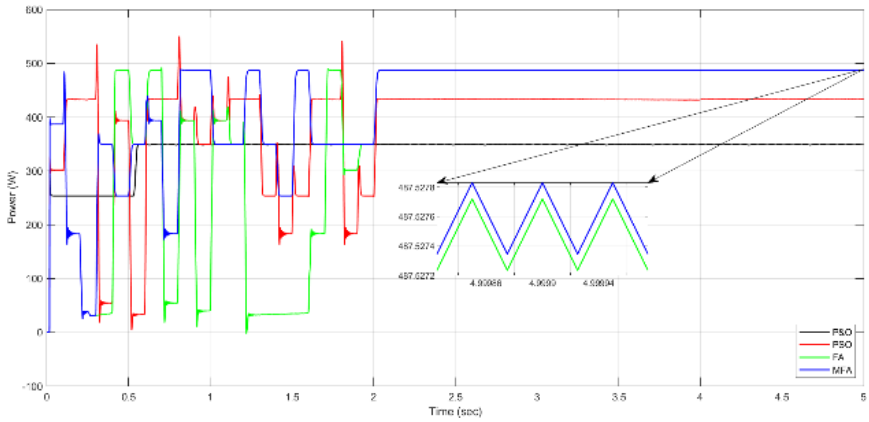

Fig. 19. Comparison of algorithms for left peak.

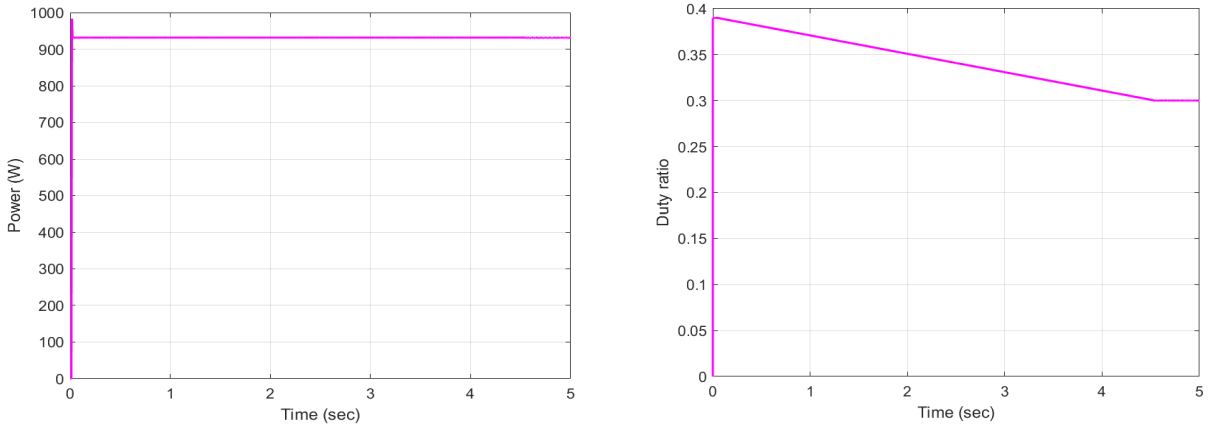

(a) PV power output (b) PWM duty ratio

Fig. 20. Right-peak P&O performance.

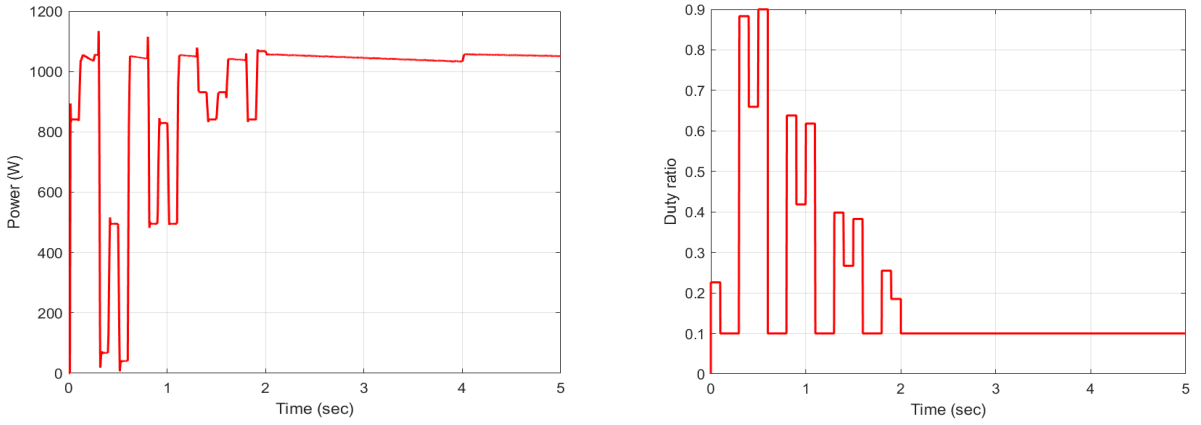

(a) PV power output (b) PWM duty ratio

Fig. 21. Right-peak PSO performance.

Fig. 22 illustrates the power output of the PV system and the corresponding duty ratio for the FA, where the generated power reaches 841.25W, with a duty cycle of approximately 0.22. However, the results indicate that the algorithm struggles to effectively track the GMPP, leading to suboptimal power extraction. In contrast, Fig. 23 presents the performance of the MFA algorithm, demonstrating a notable improvement. The generated power reaches 1.067kW, with a duty ratio of approximately 0.15, indicating a more efficient tracking capability.

For comparative analysis, Fig. 24 presents the power output of the PV system for all four algorithms. The results clearly demonstrate that MFA and PSO outperform the other two algorithms in terms of tracking efficiency and power extraction.

Among them, MFA proves to be the most effective, as it not only achieves GMPP but also converges faster and more consistently to the optimal duty ratio, ensuring stable and efficient operation under varying shading conditions.

Overall, these findings highlight MFA as the most robust and efficient MPPT algorithm, offering faster response times, greater accuracy, and superior stability in dynamic environmental conditions. MFA proves to be a highly reliable method for maximizing the efficiency of photovoltaic energy harvesting.

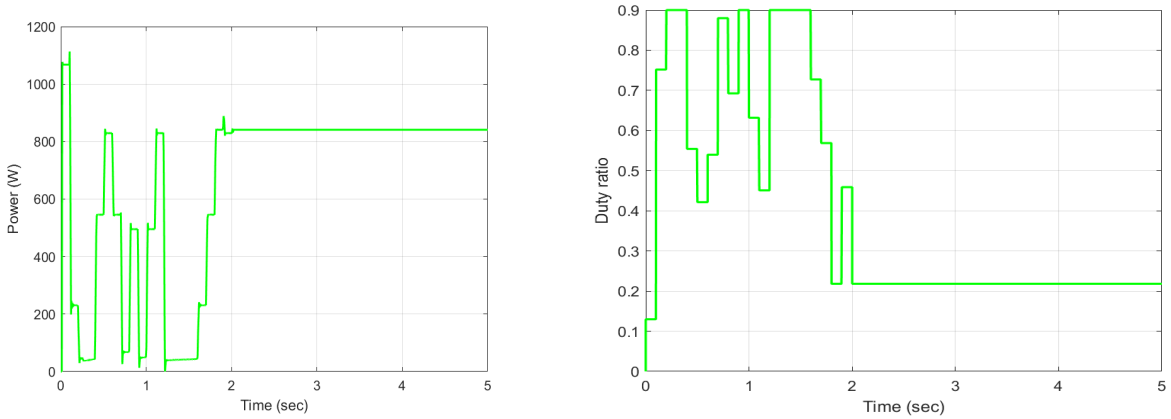

(a) PV power output (b) PWM duty ratio

Fig. 22. Right-peak FA performance.

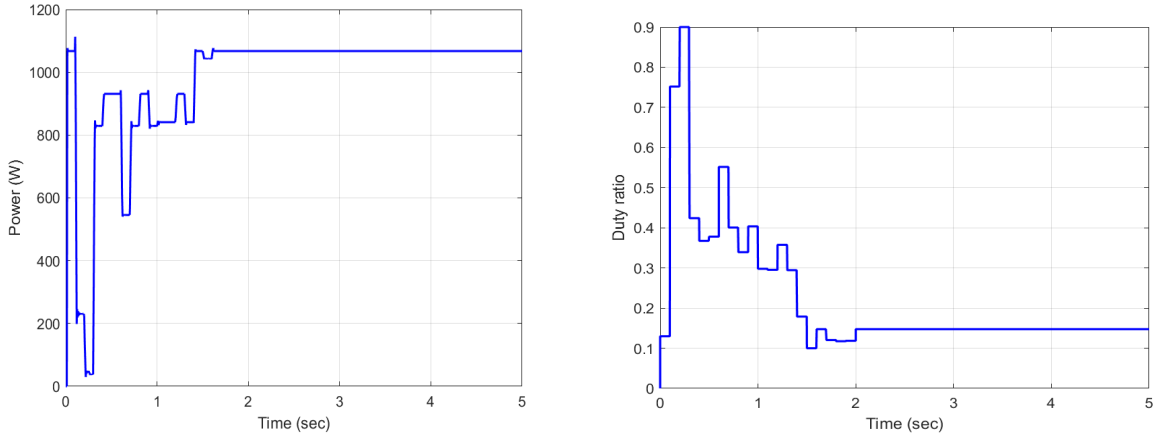

(a) PV power output (b) PWM duty ratio

Fig. 23. Right-peak MFA performance.

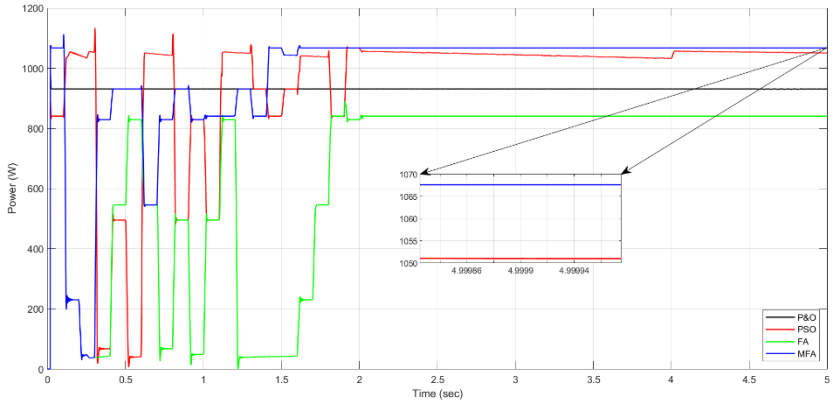

Fig. 24. Comparison of algorithms for right peak.

TABLE II presents a quantitative comparison of the four algorithms across the three partial shading conditions, with efficiency calculated based on the performance of the solar PV system. For each shading scenario, the GMPP was identified,

and the power output corresponding to each algorithm was determined through simulation. The efficiency of each algorithm was then computed as the ratio of the power output achieved by the respective MPPT controller to the ideal GMPP, as expressed in (11):

$$Efficiency(\eta) = \frac{P_{Algorithm}}{P_{GMPP}} \times 100\% \quad (11)$$

where $P_{Algorithm}$ represents the power output obtained by the MPPT algorithms, and P_{GMPP} denotes the ideal maximum power generated by the PV system.

TABLE II: Performance comparison under different PSCs.

Shading Pattern	Techniques	Power (W)	Global Maximum Power (W)	Efficiency (%)
Middle Peak	P&O	939.73	990.05	94.92
	PSO	940.29		94.97
	FA	828.89		83.72
	MFA	940.29		94.97
Left Peak	P&O	348.67	521.80	66.82
	PSO	433.78		83.13
	FA	487.53		93.43
	MFA	487.53		93.43
Right Peak	P&O	931.45	1101.58	84.56
	PSO	1051		95.40
	FA	841.25		76.37
	MFA	1067		96.86

The results emphasize the advantages of heuristic-based algorithms, PSO, FA, and MFA over conventional methods like P&O, particularly in handling multiple peaks caused by shading. While P&O achieves relatively high efficiency under middle peak conditions at 94.92%, its performance drops significantly under left peak at 66.82% due to its tendency to get stuck at local maxima. Similarly, the FA, despite being heuristic-based, underperforms compared to PSO and MFA, particularly in right peak condition, where it only achieves 76.37% efficiency, indicating poor adaptability. The MFA, by contrast, exhibits the most consistent tracking accuracy across all shading conditions, reinforcing its effectiveness as a robust MPPT strategy. These findings highlight the importance of advanced metaheuristic algorithms in optimizing the energy extraction of PV systems under real-world shading scenarios.

X. Effect of Load Resistance

The tracking efficiency of MPPT heuristic algorithms under different load resistance conditions is critical for evaluating their adaptability in real-world scenarios. To quantify the overall effectiveness the applied algorithm, the mean efficiency η_{mean} is calculated across all resistance values for each peak condition. The mean efficiency is determined using (12):

$$\eta_{mean} = \frac{1}{N}\sum_{i=1}^{N}(\eta_i) \quad (12)$$

where N is the number of resistance values considered, and η_i represents the efficiency of the algorithm at a specific resistance R_i.

- *Resistance Variation Under Middle Peak Condition:*

The performance of MPPT under varying resistances for the middle peak condition is illustrated in the figures below. Fig. 25 presents the performance of PSO, while Fig. 26 and Fig. 27 depict the performance of FA and MFA, respectively.

TABLE III: Resistance variation under middle peak condition.

R_i (Ω)	PSO		FA		MFA	
	P (W)	η_i	P (W)	η_i	P (W)	η_i
20	940.29	94.97%	828.89	83.72%	940.29	94.97%
30	916.05	92.53%	916.05	92.53%	916.05	92.53%
40	610.46	61.66%	988.64	99.86%	988.64	99.86%
50	752.51	76.01%	874.27	88.31%	874.27	88.31%
60	891.13	90.01%	891.13	90.01%	891.13	90.01%
70	989.06	99.90%	989.06	99.90%	989.06	99.90%
η_{mean}	85.85%		92.39%		94.26%	

For the middle peak condition, the mean efficiency values were 85.85% for PSO, 92.39% for FA, and 94.26% for MFA. The PSO algorithm exhibited fluctuating efficiency, dropping as low as 61.66% for R=40Ω but recovering at higher resistances. FA demonstrated more stable performance, maintaining efficiency values consistently above 83.72% and reaching a peak efficiency of 99.90% at R=70Ω. The MFA algorithm achieved the highest mean efficiency, maintaining values above 88.31% across all resistances and peaking at 99.90% for R=70Ω. This confirms MFA's superior adaptability in tracking the maximum power under the given shading condition. TABLE III presents the impact of different load resistances on the middle peak condition.

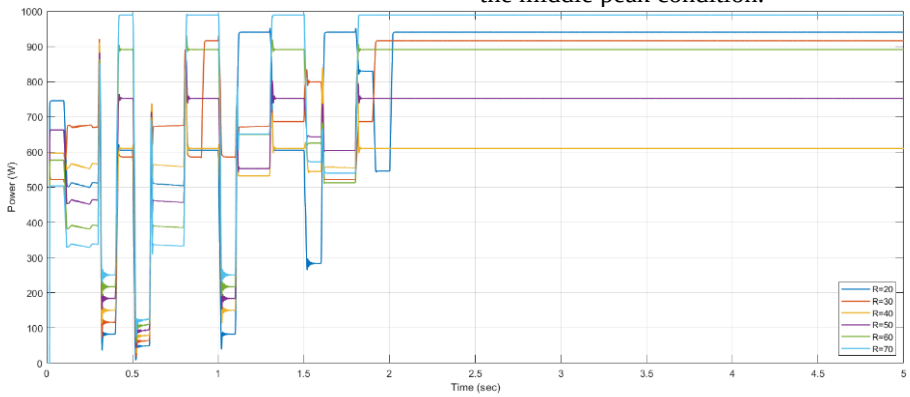

Fig. 25. PSO algorithm for different values of R under the middle peak condition.

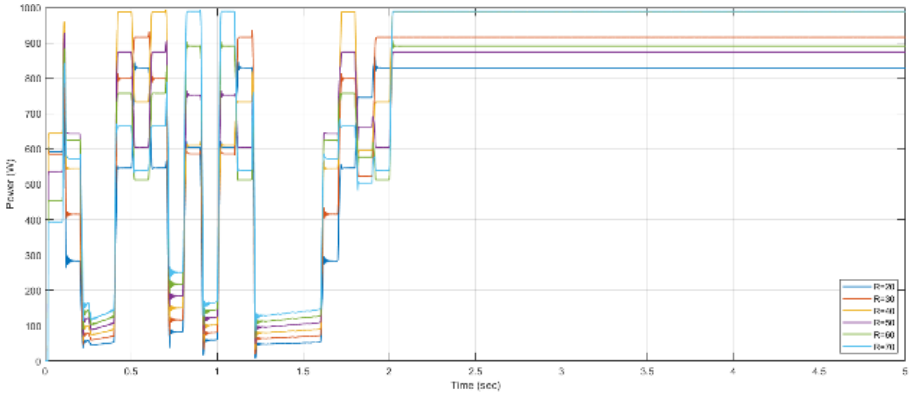

Fig. 26. FA algorithm for different values of R under the middle peak condition.

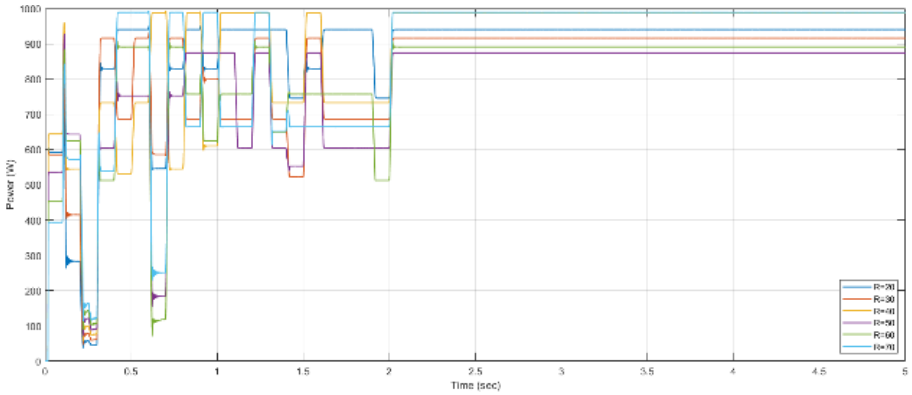

Fig. 27. MFA algorithm for different values of R under the middle peak condition.

- *Resistance Variation Under Left Peak Condition:*

The performance of MPPT under varying resistances for the left peak condition is illustrated in the figures below. Fig. 28 presents the performance of PSO, while Fig. 29 and Fig. 30 depict the performance of FA and MFA, respectively. For the left peak condition, the mean efficiency values were 85.57% for PSO, 93.26% for FA, and 93.26% for MFA. The PSO algorithm exhibited noticeable fluctuations, with efficiency dropping to 77.30% at R=70Ω, highlighting its sensitivity to changes in load resistance. In contrast, FA and MFA demonstrated significantly better tracking performance, with efficiency values consistently exceeding 93% across most resistances and peaking at 99.83% for R=30Ω. The similarity in FA and MFA performance in this condition suggests that both algorithms are well-suited for tracking MPP when shading patterns result in left-dominant peaks in the P-V curve. TABLE IV presents the impact of different load resistances on the left peak condition.

TABLE IV: Resistance variation under left peak condition.

R_i (Ω)	PSO		FA		MFA	
	P (W)	η_i	P (W)	η_i	P (W)	η_i
20	433.78	83.13%	487.53	93.43%	487.53	93.43%
30	520.92	99.83%	520.92	99.83%	520.92	99.83%
40	451.44	86.52%	451.44	86.52%	451.43	86.51%
50	435.50	83.46%	435.50	83.46%	435.50	83.46%
60	434.14	83.20%	507.24	97.21%	507.24	97.21%
70	403.33	77.30%	517.19	99.12%	517.19	99.12%
η_{mean}	85.57%		93.26%		93.26%	

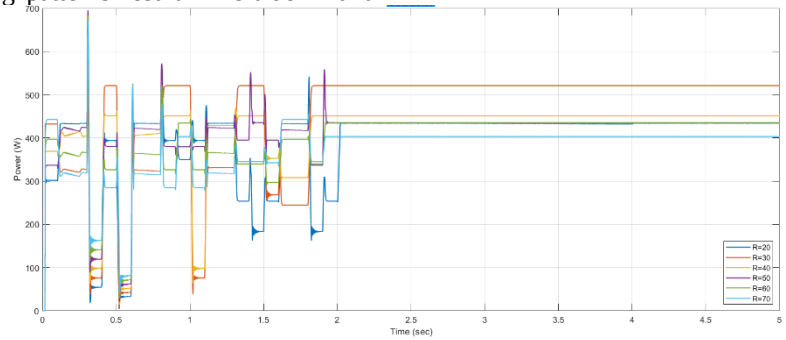

Fig. 28. PSO algorithm for different values of R under the left peak condition.

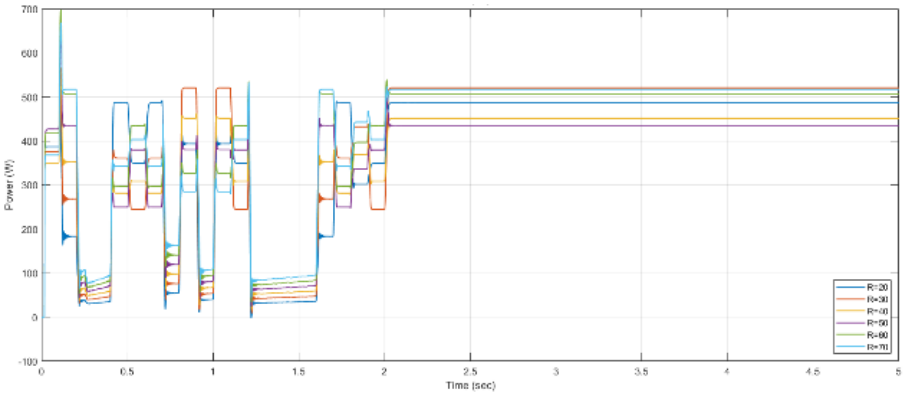

Fig. 29. FA algorithm for different values of R under the left peak condition.

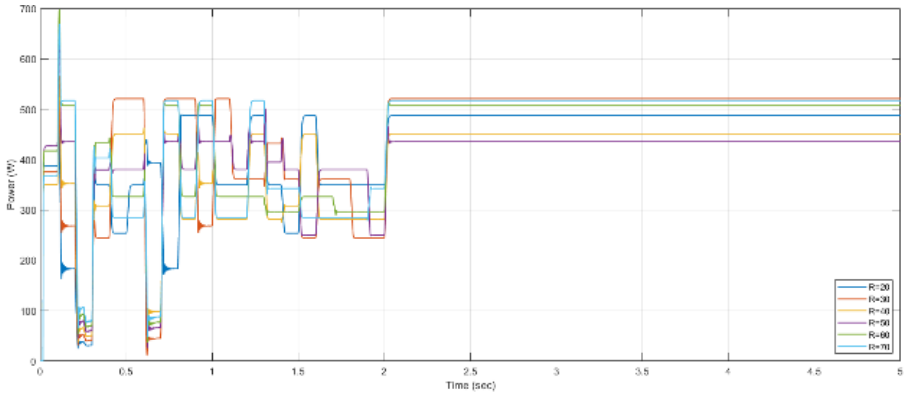

Fig. 30. MFA algorithm for different values of R under the left peak condition.

- *Resistance Variation Under Right Peak Condition:*

The performance of MPPT under varying resistances for the right peak condition is illustrated in the figures below. Fig. 31 presents the performance of PSO, while Fig. 32 and Fig. 33 depict the performance of FA and MFA, respectively. For the right peak condition, the mean efficiency values were 88.39% for PSO, 90.41% for FA, and 95.35% for MFA. The PSO algorithm exhibited high efficiency at R=40Ω, achieving 98.13%, but experienced notable drops at lower and higher resistances, such as 83.43% at R=30Ω and 80.84% at R= 60Ω, indicating its sensitivity to resistance variations. FA demonstrated improved consistency, particularly at moderate resistances, with a peak efficiency of 97.02% at R=30Ω, maintaining values above 89% across the range. MFA outperformed both algorithms, achieving the highest mean efficiency among the three. Notably, it maintained efficiency above 95% for most resistances, reaching 98.13% at R=40Ω and 95.84% at R=60Ω, reaffirming its robustness and ability to accurately track the GMPP. TABLE V presents the impact of different load resistances on the right peak condition.

TABLE V: Resistance variation under left peak condition.

R_i (Ω)	PSO		FA		MFA	
	P (W)	η_i	P (W)	η_i	P (W)	η_i
20	1051.00	95.41%	841.25	76.37%	1067.00	96.86%
30	919.04	83.43%	1068.80	97.02%	1068.80	97.02%
40	1081.00	98.13%	980.40	89.00%	1081.00	98.13%
50	919.01	83.43%	1048.10	95.15%	1048.10	95.15%
60	890.53	80.84%	1055.80	95.84%	1055.80	95.84%
70	981.58	89.11%	981.58	89.11%	981.58	89.11%
η_{mean}	88.39%		90.41%		95.35%	

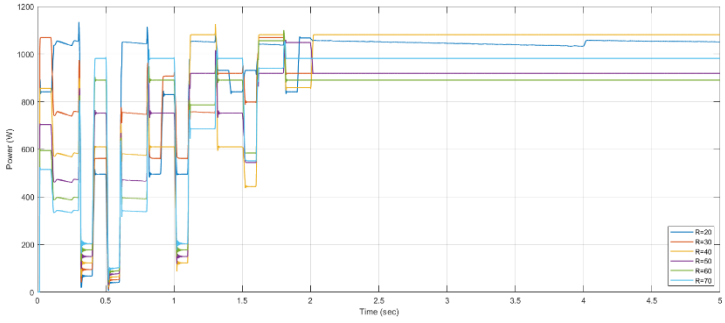

Fig. 31. PSO algorithm for different values of R under the right peak condition.

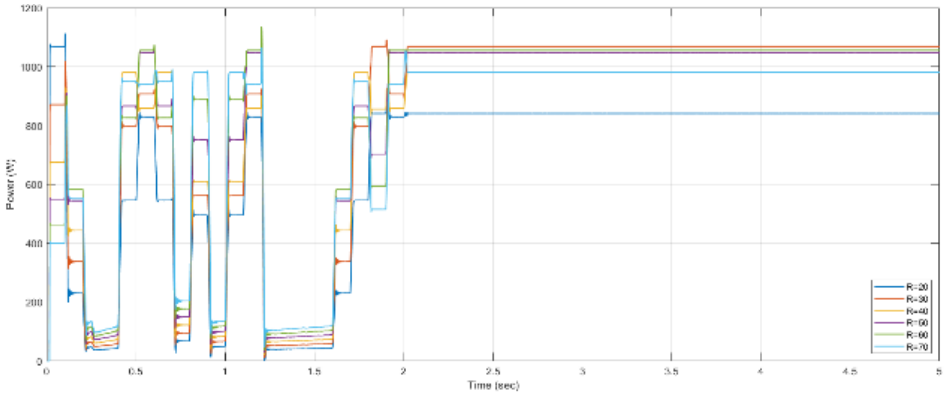

Fig. 32. FA algorithm for different values of R under the right peak condition.

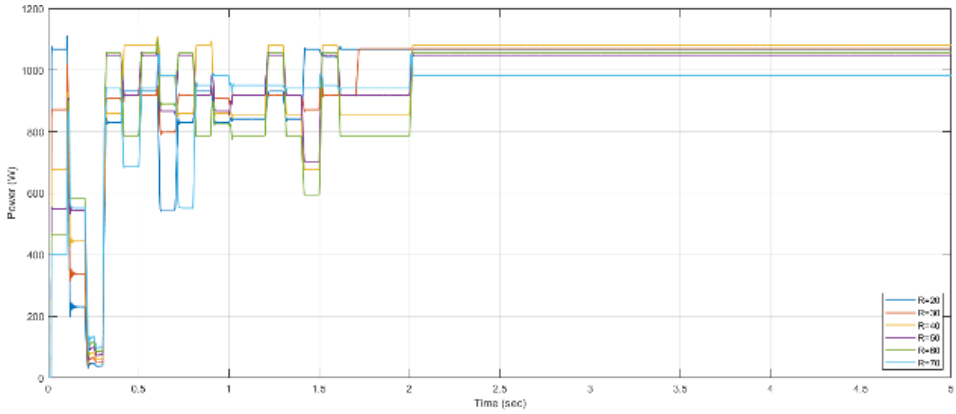

Fig. 33. MFA algorithm for different values of R under the right peak condition.

XI. Conclusion

The comparative analysis conducted in this study underscores the effectiveness of the Modified Firefly Algorithm (MFA) in tracking the Maximum Power Point (MPP) under Partial Shading Conditions (PSC) in photovoltaic (PV) systems. Through extensive simulations, MFA consistently outperformed the conventional Perturb and Observe (P&O) algorithm, as well as the metaheuristic approaches Particle Swarm Optimization (PSO) and the standard Firefly Algorithm (FA), across all tested shading patterns. While FA exhibited stable tracking capabilities, MFA's adaptive parameter tuning enabled it to achieve higher mean efficiency, particularly in scenarios where PSO experienced efficiency drops due to variations in load resistance.

Furthermore, MFA showed remarkable consistency in maintaining high efficiency while adjusting to different resistances, demonstrating its robustness and adaptability in dynamic environmental conditions. The findings indicate that, although PSO and FA occasionally approached MFA's performance under certain conditions, they were unable to maintain the same level of efficiency across all scenarios. MFA's ability to efficiently converge toward the global MPP while minimizing fluctuations makes it the most reliable MPPT algorithm among the tested methods.

Overall, the results of this study confirm that MFA is the most efficient and adaptive algorithm for optimizing power extraction in PV systems under varying shading and load conditions. Its superior tracking performance, faster convergence, and ability to maintain high efficiency in all cases reinforce its potential as a leading solution for enhancing the reliability and efficiency of solar energy systems.

References

[1] T. T. Yetayew, T. R. Jyothsna, and G. Kusuma, "Evaluation of Incremental conductance and Firefly algorithm for PV MPPT application under partial shade condition," 2016 IEEE 6th Int. Conf. Power Syst. ICPS 2016, pp. 0–5, 2016, doi: 10.1109/ICPES.2016.7584089.

[2] M. Sameeullah and A. Swarup, "MPPT schemes for PV system under normal and partial shading condition: A review," Int. J. Renew. Energy Dev., vol. 5, no. 2, pp. 79–94, 2016, doi: 10.14710/ijred.5.2.79-94.

[3] Y. Zhang, Y. J. Wang, H. Li, J. B. Chang, and J. Q. Yu, "A Firefly Algorithm and Elite Ant System-Trained Elman Neural Network for MPPT Algorithm of PV Array," Int. J. Photoenergy, vol. 2022, 2022, doi: 10.1155/2022/5700570.

[4] Y. Huang, M. Huang, and C. Ye, "Propagation for Photovoltaic MPPT Under," vol. 11, no. 4, pp. 2641–2652, 2020.

[5] N. A. Windarko, A. Tjahjono, D. O. Anggriawan, and M. H. Purnomo, "Maximum power point tracking of photovoltaic system using adaptive modified firefly algorithm," Proc. - 2015 Int. Electron. Symp. Emerg. Technol. Electron. Information, IES 2015, pp. 31–35, 2016, doi: 10.1109/ELECSYM.2015.7380809.

[6] D. F. Teshome, C. H. Lee, Y. W. Lin, and K. L. Lian, "A modified firefly algorithm for photovoltaic maximum power point tracking control under

partial shading," IEEE J. Emerg. Sel. Top. Power Electron., vol. 5, no. 2, pp. 661–671, 2017, doi: 10.1109/JESTPE.2016.2581858.

[7] R. B. A. Koad, A. F. Zobaa, and A. El-Shahat, "A Novel MPPT Algorithm Based on Particle Swarm Optimization for Photovoltaic Systems," IEEE Trans. Sustain. Energy, vol. 8, no. 2, pp. 468–476, 2017, doi: 10.1109/TSTE.2016.2606421.

[8] T. L. Nguyen and K. S. Low, "A global maximum power point tracking scheme employing DIRECT search algorithm for photovoltaic systems," IEEE Trans. Ind. Electron., vol. 57, no. 10, pp. 3456–3467, 2010, doi: 10.1109/TIE.2009.2039450.

[9] L. N. Palupi, T. Winarno, A. Pracoyo, and L. Ardhenta, "Adaptive voltage control for MPPT-firefly algorithm output in PV system," IOP Conf. Ser. Mater. Sci. Eng., vol. 732, no. 1, 2020, doi: 10.1088/1757-899X/732/1/012048.

[10] S. S. Mohammed, D. Devaraj, and T. P. I. Ahamed, "Maximum power point tracking system for stand alone solar PV power system using Adaptive Neuro-Fuzzy Inference System," 2016 - Bienn. Int. Conf. Power Energy Syst. Towar. Sustain. Energy, PESTSE 2016, no. September 2019, 2016, doi: 10.1109/PESTSE.2016.7516536.

[11] A. G. Abo-Khalil, W. Alharbi, A. R. Al-Qawasmi, M. Alobaid, and I. M. Alarifi, "Maximum power point tracking of PV systems under partial shading conditions based on opposition-based learning firefly algorithm," Sustain., vol. 13, no. 5, pp. 1–18, 2021, doi: 10.3390/su13052656.

[12] S. M. Sulthan, D. Devaraj, S. R. B., M. M. O., and V. Raj, "Development and analysis of a Two stage Hybrid MPPT algorithm for solar PV systems," Energy Reports, vol. 9, pp. 1502–1512, 2023, doi: 10.1016/j.egyr.2023.07.006.

[13] M. Seyedmahmoudian R. Rahmani, S. Mekhilef, A. Stojcevski, T. Soon, A. Ghandhari, "Simulation and Hardware Implementation of New Maximum Power Point Tracking Technique for Partially Shaded PV System Using Hybrid DEPSO Method," IEEE Trans. Sustain. Energy, vol. 6, no. 3, pp. 850–862, 2015, doi: 10.1109/TSTE.2015.2413359.

[14] W. Hayder, E. Ogliari, A. Dolara, A. Abid, M. Ben Hamed, and L. Sbita, "Improved PSO: A comparative study in MPPT algorithm for PV system control under partial shading conditions," Energies, vol. 13, no. 8, 2020, doi: 10.3390/en13082035.

[15] S. Hesari, "Design and implementation of maximum solar power tracking system using photovoltaic panels," Int. J. Renew. Energy Res., vol. 6, no. 4, pp. 1221–1226, 2016, doi: 10.20508/ijrer.v6i4.4352.g6909.

[16] D. P and K. R. Kumar, "Mppt Based Control of Sepic Converter Using Firefly Algorithm for," pp. 1–8, 2017.

[17] A. I. Nusaif and A. L. Mahmood, "MPPT Algorithms (PSO, FA, and MFA) for PV System Under Partial Shading Condition, Case Study: BTS in Algazalia, Baghdad," Int. J. Smart grid, no. September, 2020, doi: 10.20508/ijsmartgrid.v4i3.113.g99.

[18] J. Farzaneh, R. Keypour, and M. A. Khanesar, "A New Maximum Power Point Tracking Based on Modified Firefly Algorithm for PV System Under Partial Shading Conditions," Technol. Econ. Smart Grids Sustain. Energy, vol. 3, no. 1, 2018, doi: 10.1007/s40866-018-0048-7.

[19] M. Agdam, A. Asbayou, M. Elyaqouti, A. Ihlal, and K. Assalaou, "MPPT of PV System Under Partial Shading Conditions Based on Bio-inspired Swarm Intelligence Technique," E3S Web Conf., vol. 297, pp. 1–6, 2021, doi: 10.1051/e3sconf/202129701051.

[20] A. Gil-Velasco and C. Aguilar-Castillo, "A modification of the perturb and observe method to improve the energy harvesting of pv systems under partial shading conditions," Energies, vol. 14, no. 9, 2021, doi: 10.3390/en14092521.

[21] M. S. Nkambule, A. N. Hasan, and A. Ali, "MPPT under partial shading conditions based on Perturb & Observe and Incremental Conductance," ELECO 2019 - 11th Int. Conf. Electr. Electron. Eng., pp. 85–90, 2019, doi: 10.23919/ELECO47770.2019.8990426.

[22] A. Pandey and S. Srivastava, "Perturb & Observe MPPT Technique used for PV System Under different Environmental Conditions," Int. Res. J. Eng. Technol., vol. 06, no. 04, pp. 2829–2835, 2019, [Online]. Available: www.irjet.net

[23] J. García-Morales, G. Femenias, and F. Riera-Palou, "Analysis and Optimization of FFR-Aided OFDMA-Based Heterogeneous Cellular Networks," IEEE Access, vol. 4, pp. 5111–5127, 2016, doi: 10.1109/ACCESS.2016.2599026.

[24] M. Rehan and M. M. A. Awan, "Optimization of MPPT perturb and observe algorithm for a standalone solar PV system," Mehran Univ. Res. J. Eng. Technol., vol. 43, no. 3, p. 136, 2024, doi: 10.22581/muet1982.3147.

[25] E. W. Mukti, A. Risdiyanto, A. A. Kristi, and R. Darussalam, "Particle Swarm Optimization (PSO) based Photovoltaic MPPT Algorithm under the Partial Shading Condition," J. Elektron. dan Telekomun., vol. 23, no. 2, p. 99, 2023, doi: 10.55981/jet.552.

[26] A. Lakhdara, T. Bahi, and A. Moussaoui, "PSO Control under Partial Shading Conditions," Alger. J. Renew. Energy Sustain. Dev., vol. 2, no. 02, pp. 126–136, 2020, doi: 10.46657/ajresd.2020.2.2.5.

[27] M. Sababha, M. Zohdy, and M. Kafafy, "The enhanced firefly algorithm based on modified exploitation and exploration mechanism," Electron., vol. 7, no. 8, 2018, doi: 10.3390/electronics7080132.